

The thermal capillary migration properties and controlling technique of ferrofluids

Proc IMechE Part J:
J Engineering Tribology
2017, Vol. 231(11) 1441–1449
© IMechE 2017
Reprints and permissions:
sagepub.co.uk/journalsPermissions.nav
DOI: 10.1177/1350650117698630
journals.sagepub.com/home/pij



Qingwen Dai¹, Wei Huang¹, Jingqiu Wang¹ and Xiaolei Wang^{1,2}

Abstract

The thermal capillary migration describes a phenomenon where the thermal gradients on the surface drive a liquid to flow from warm to cold regions in the absence of external forces. In industry, it is of great importance to prevent the migration since it would lead to lubricant starvation on the moving components. In this paper, ferrofluids are employed to control the migration. The influence of external magnetic field on the migration of ferrofluids is studied. The effects of volume and saturation magnetization of ferrofluids are also investigated. Experimental results demonstrate that the external magnetic field intensities have a significant obstruction effect on the migration behavior. An effective method using electromagnet to control the migration and re-concentrate the migrated lubricant is proposed.

Keywords

Thermal capillary migration, ferrofluids, external magnetic field, lubricant re-concentration

Date received: 7 July 2016; accepted: 9 February 2017

Introduction

The motion of a liquid droplet on a horizontal solid surface induced by thermal gradients has been reported long ago.^{1–4} It essentially refers to a phenomenon of thermal capillary migration where the variation of interfacial tension caused by temperature differences drives the droplet to move from a high-temperature locale to an area of relatively low temperature.^{5–7} This migration has received abundant attentions for its significant influences in the lubrication of space mechanisms,^{8–10} ball bearings,¹¹ and magnetic recording media.¹² Since on these moving components, spontaneous heat generated by the friction will create a thermal gradient on the contact area and induce the lubricant migration, resulting in lubricant starvation in the friction region. Therefore, the controlling of the migration behavior is a key issue to ensure effective lubrication.

In most of the strategies, the geometrical anisotropy and wettability gradient can be the effective manners to regulate the liquid migration on a surface.^{13–15} Generally, an aligned structure can restrict the migration easily in the perpendicular direction, but guide the motion of the liquid in the parallel direction;^{16–19} isotropic structures of microdimples patterns,^{20,21} and low surface energy coatings around rubbing region,²² can obstruct the omnidirectional migration effectively. In addition, liquid lubricants

with low viscosity are prone to migrate. Thus, lubricants with high viscosities are usually employed to prevent the migration.²³

Ferrofluids (FF) are a colloidal system consisting of single domain ferromagnetic particles dispersed in a carrier liquid.^{24–26} The nanoparticles have a mean diameter of about 10 to 20 nm, and the surfactant is adsorbed around each particle to provide a short-range steric repulsion between particles preventing particle agglomeration. FF is a homogeneous liquid and widely served as the liquid lubricant in space and vacuum conditions, helping enhance the lubrication effect, reducing dosage of lubricant, and preventing leakage.^{27–29}

More importantly, FF can be magnetized by applying an external magnetic field and maintain the properties of the fluid simultaneously. With an appropriate magnetic field intensity, it can be confined, positioned, and controlled at a designated area. So, could this

¹College of Mechanical and Electrical Engineering, Nanjing University of Aeronautics & Astronautics, Nanjing, China

²Jiangsu Key Laboratory of Precision and Micro-Manufacturing Technology, Nanjing, China

Corresponding author:

Xiaolei Wang, College of Mechanical and Electrical Engineering, Nanjing University of Aeronautics & Astronautics, 29# Yudao Street, Nanjing 210016, China.

Email: wxl@nuaa.edu.cn

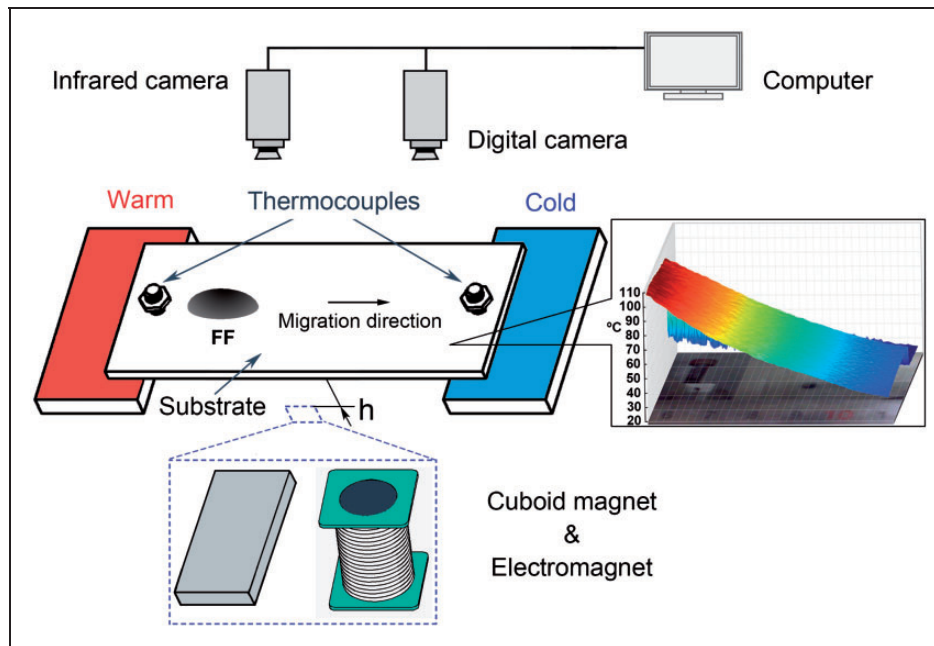


Figure 1. The schematic diagram of the experimental apparatus.

mechanism be applied to control the migration in the lubrication assembly, in which the volume of lubricant is limited and the migration must be taken into consideration? During the migration process, what is the relationship between the FF migration and the magnetic field intensity? When the migration has already occurred, can this mechanism be used to design a magnetic switch to re-concentrate the migrated lubricant?

Therefore, in this paper, thermal gradient induced migration of the FF droplet was studied. The effect of external magnetic field on the thermocapillary migration of FF was investigated. Particular attention was paid to the function of electromagnet on the migration behavior. A magnetic switch to control the migration and re-concentrate the migrated lubricant is proposed.

Experimental section

Figure 1 shows the schematic diagram of the apparatus used in this study. Thermal capillary migration was experimented on a substrate of SUS 316 nonmagnetic stainless steel. The substrates were fabricated with dimensions of $76 \text{ mm} \times 30 \text{ mm} \times 3 \text{ mm}$ with an average surface roughness Ra of 20 nm. Two temperature-controlled elements were tightly attached to the ends of the substrate. The cold side was maintained at a constant temperature of 0°C , and by changing the temperature of the warm side, a thermal gradient could be generated along the length of the surface. An infrared camera (Fluke, USA) was used to obtain the thermography on the substrate surface. As shown in Figure 1, the thermography confirmed that the thermal gradient was nearly linear along the length direction of the substrate surface, and the

average value was used in this study. A digital video camera was employed to monitor the dynamic migration process. From the location of the front edge of the droplet in the successive images, the migration distance and the average velocity curve could be obtained.

To generate a stable magnetic field on the substrate surface, a cuboid NdFeB permanent magnet (dimensions of $60 \text{ mm} \times 20 \text{ mm} \times 5 \text{ mm}$, property: 36 MGOe) was placed under the substrate with a variable gap (h). Moreover, to generate a changeable magnetic field intensity, an electromagnet was also employed and placed under the substrate with a given gap. Through adjusting the exciting current in the coils of the electromagnet, the magnetic field intensity could be changed at any moment.

Prior to the experiments, the substrates were ultrasonically cleaned with acetone and alcohol, rinsed with deionized water, and blow-dried with nitrogen. When the set thermal gradient was reached, an FF droplet with a certain volume was dropped at the warm side via a microliter syringe. For the FF used in this study, the Fe_3O_4 nanoparticles coated with an ashless dispersant surfactant, T161 (high molecular weight succinimides), were dispersed in the carrier lubricant of α -olefinic hydrocarbon synthetic oil (PAO4) via the ultrasonic method. The content of T161 was 6 wt%. The properties of the carrier liquid and FF were given in Table 1. The test conditions of lubricant migration were shown in Table 2.

In order to determine the migration properties of FF, the migration behavior of the carrier liquid, carrier liquid with surfactant (PAO4+ 6 wt% T161) and FF were experimented firstly. Then, the migration properties of FF under an external magnetic field generated by a cuboid magnet or an electromagnet

Table 1. Properties of carrier liquid and ferrofluids (FF) at 20°C.

Liquid	Density (kg/m ³)	Viscosity (mPa·s)	Saturation magnetization (kA/m)
Carrier liquid (PAO4)	0.84×10^3	50	0
FF-1	1.05×10^3	67	15.9
FF-2	1.21×10^3	95	31.8

Table 2. Experimental conditions.

Environment temperature	20°C
Thermal gradient	2, 2.6, 3.2°C/mm
Gap between substrate and magnet (<i>h</i>)	2, 9, and 15 mm
Gap between substrate and electromagnet (<i>h</i>)	2 mm
Volume of lubricant	5 μL, 10 μL

Table 3. Surface tensions of the tested lubricants at different temperatures.

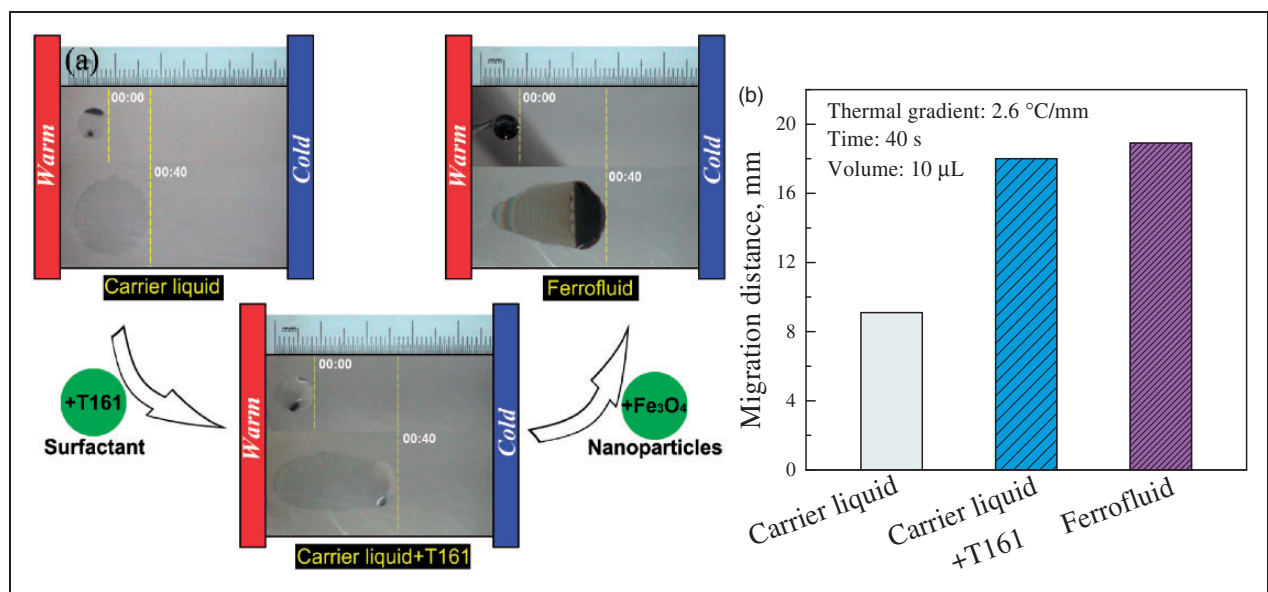
Lubricants	Surface tensions (mN/m)			
	20°C	40°C	60°C	80°C
PAO4	26.589	24.122	22.869	21.696
PAO4+ 6 wt% T161	29.157	27.661	26.104	24.466
FF-1	27.277	25.336	23.799	22.485
FF-2	27.256	25.376	23.900	22.788

were investigated. Meanwhile, the surface tensions of the tested lubricants was measured via the Wilhelmy plate method, and the detailed data of the surface tensions were shown in Table 3.

Results and discussion

Figure 2(a) provides key frames, with a time interval of 40 s, showing the migration behavior of the carrier liquid, carrier liquid with surfactant and FF-1 on the smooth surface. The volume of FF is 10 μL and the thermal gradient is 2.6°C/mm. The migration distances of those liquids are shown in Figure 2(b). For the carrier liquid, the droplet migrates in a short distance towards the cold side, accompanying with a diffusion process to the surroundings. When the carrier liquid is mixed with T161 (content of 6 wt%), it is interesting that the liquid migrates in a quite long distance, approximately 18 mm, which is nearly 200% longer than the 9.1 mm observed for the pure carrier liquid. Moreover, for the droplet of FF-1, it migrates in a distance about 19 mm, which is a bit longer compared with that of the carrier liquid+T161.

It is known that T161 is a sort of high-performance ashless dispersant. Chemically, this dispersant contains abundant polar groups, which is also regarded as a surfactant. Our previous research has demonstrated that adding T161 into a base oil will increase the surface tension and accelerate the migration of lubricant.³⁰ Therefore, on one hand, when the carrier liquid mixed with T161, the surface tension is increased (Table 3), which promotes the migration behavior and resulting in a longer migration distance than the pure one. On the other hand, for the FF used

**Figure 2.** (a) The detailed thermal gradient induced migration process of carrier liquid, carrier liquid with surfactant, and FF on a smooth surface. (b) Comparison of the migration distances of those three liquids.

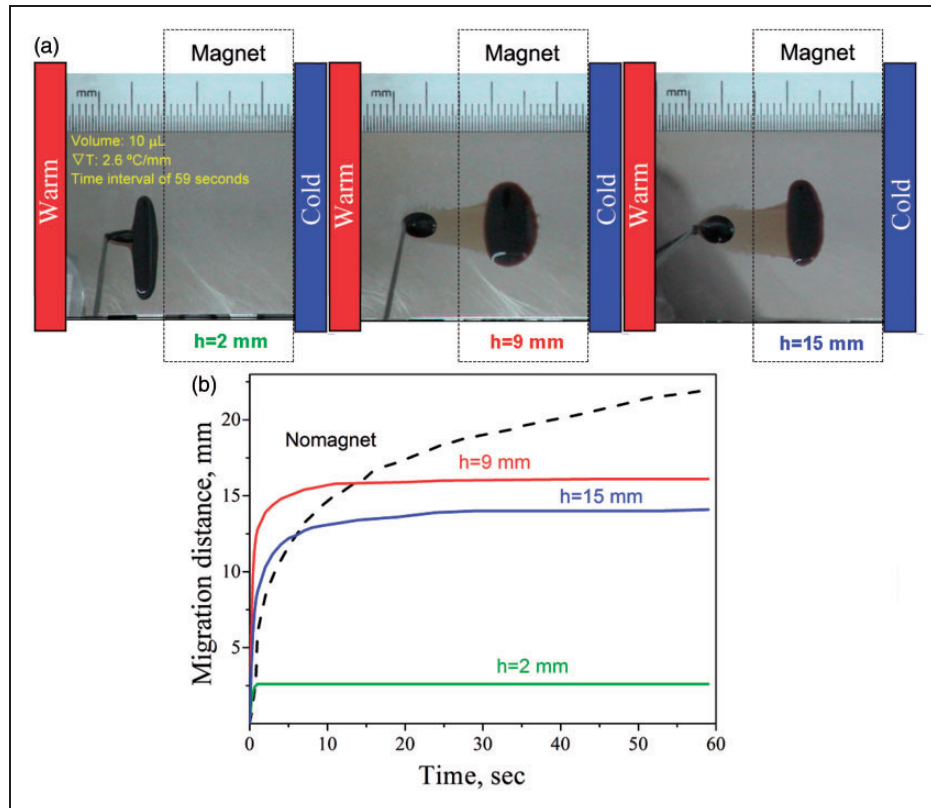


Figure 3. (a) Migration process of the FF-1 droplets on a smooth surface with different external magnetic field intensities. (b) Migration distance versus elapsed time under these three magnetic field intensities.

in this study, this dispersant is indispensable since it is chiefly used for improving the dispersion performance of the nanoparticles in the carrier liquid and enhancing the stability of FF. Therefore, in order to obstruct the migration of FF, an external magnetic field is applied and the migration behavior is investigated in the following sections.

A permanent magnet is situated under the substrate and the gap (h) between the two surfaces is set at 2 mm, 9 mm, and 15 mm, generating three different magnetic field intensities on the surface. Figure 3(a) exhibits the migration processes of the FF-1 droplet with a volume of $10 \mu\text{L}$ under a thermal gradient of $2.6^\circ\text{C}/\text{mm}$. Each sub-image is a superimposed image consisting of two video frames recorded with the time interval of 59 s. The detailed migration distances are shown in Figure 3(b). Under the gap (h) of 2 mm, the thermal gradient yields a very short migration distance, and just within 1 s, the droplet is absorbed stationary at this position, unable to migrate. When the gap (h) is increased to 9 mm, the thermal gradient yields a migration distance about 16.1 mm, which is much longer than that of $h = 2$ mm; as the gap (h) further increases to 15 mm, the migration distance is decreased a little, about 14.1 mm.

In comparison to the migration distance on the surface with no magnetic field, which is always increased with time elapsing, these experimental results demonstrate that an external magnetic field

can restrict the migration behavior and positioned the FF droplet at one position.

Definitely, the variation of migration distances is attributable to the magnetic force induced by the external magnetic field. The external magnetic field produces attractive forces on the particles in the fluid. The unit volume value of the induced magnetic force (F_m) for nonconductive FF can be expressed as³¹

$$F_m = \mu_0 \chi_m H \cdot \nabla H \quad (1)$$

where μ_0 is the magnetic permeability of vacuum, χ_m is the susceptibility of FF, ∇H is the magnetic field intensity, and ∇H represents the gradient of the magnetic field.

The surface magnetic intensities (H) generated by the cuboid NdFeB permanent magnet with various gaps (h) of 2, 9, and 15 mm were calculated via the Ansoft Maxwell 14.0 software. Figure 4(a) shows the magnetic field distribution on the surface of the substrate, and Figure 4(b) shows the surface magnetic intensity (H) at the substrate centerline in the length direction (as illustrated in the inset figure).

When the gap (h) equaled to 2 mm, the magnet yields a considerable high surface magnetic intensity (H) on the surface, and the maximum surface magnetic intensity (H) appears at the region upon the center where the cuboid magnet is fixed, as high as

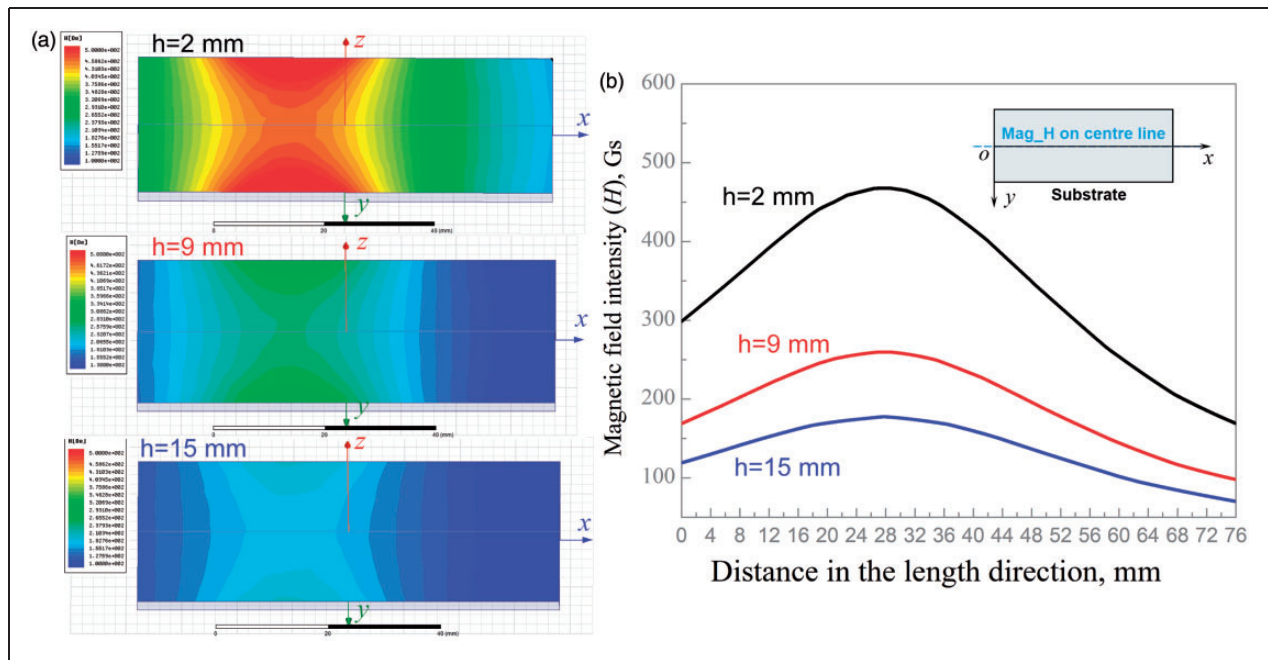


Figure 4. (a) The surface magnetic intensity (H) distribution diagrams on the surface of the substrate with a variation gap h . (b) The surface magnetic intensity (H) at the centerline direction of the substrate surface.

470 Gs. According to equation (1), the interaction between the magnetic field and FF increases with the increase in the surface magnetic intensity (H) and the gradient of magnetic field (∇H). The generated magnetic force is too strong to liberate the droplet to move, so the droplet was tightly adsorbed on the surface, just migrated in a very short distance. Moreover, it can be found that there exists a positive gradient of magnetic field (∇H) in the vertical direction; this will produce a vertical magnetic force on the droplet dragging it spreading in the vertical direction. That is the reason why the droplet formed a strip shape as the experimental result shown in Figure 3(a) ($h=2$ mm).

Actually, both the magnetic forces while $h=9$ mm and $h=15$ mm at the central position right above the magnet are large enough to confine the FF, therefore, there is just a little difference between the migration distances of $h=9$ mm and $h=15$ mm. Since the magnetic force (F_m) is also proportional to the gradient of magnetic field (∇H), as the calculated surface magnetic intensity distribution of $h=9$ mm and $h=15$ mm shown in Figure 4, the gradient of magnetic field (∇H) of $h=9$ mm is larger than that of $h=15$ mm, which produces a larger vertical magnetic force on the droplet, dragging it spreading to the surroundings. As a consequence, the migration distance of $h=9$ mm is a bit longer.

Inspired by the fact that an external magnetic field could restrict the migration behavior, a magnetic switch is designed to control the migration and re-concentrate the migrated lubricant. An electromagnet is employed and placed right under the substrate with a gap of 2 mm, as the yellow dotted circle

illustrated in Figure 5(a) and (b). The droplets are placed at two different positions on the substrate surface. The thermal gradient is $2^\circ\text{C}/\text{mm}$ and the volume of the FF-1 droplet is $5 \mu\text{L}$.

In case I, as illustrated in Figure 5(a), there is no current when the droplet is placed on the surface. Under the effect of thermal gradient, the droplet is permitted to migrate to the cold side for 95 s. Then, as the electromagnet is switched on, the migrated droplet returns back rapidly, against the thermal capillary force, and just within 3 s, the droplet is firmly controlled at the area right upon the electromagnet and unable to migrate anymore. Only after the electromagnet is switched off again, the droplet can re-migrate to the cold side.

In case II, as illustrated in Figure 5(b), the droplet is placed right upon the switched on electromagnet. The magnetic force is large enough so that the droplet cannot move, and only after switching off the electromagnet, the droplet is released to migrate to the cold side. Once again, with switching on, the migrated droplet moves backward without hesitation, and it can be re-concentrated at the initial location. Moreover, these processes are repeatable.

Figure 5(a') and (b') shows the migration distances of the FF-1 droplet in these two cases. The migration, re-concentration, and re-migration phenomena induced by the repeated processes of switching off and switching are quantitatively exhibited. It is clearly shown that the droplet can be re-concentrated at the location as long as possible in these two cases. A magnetic switch to control the migration and re-concentrate the migrated droplet is achieved. In case II, the droplet migrated in a relatively negative

direction during the re-concentration process, as shown in Figure 5(b'). That is because the starting position is defined as the front edge of the droplet where it was first placed.

Figure 5(c) shows the surface magnetic intensity (H) at z direction right above the electromagnet center (as the inset figure shown). When z is 2 mm, the surface magnetic intensity (H) is about 384 Gs, and the surface magnetic intensity (H) decreases with increasing z . Figure 5(d) shows the surface magnetic intensity (H) at x direction on the substrate surface (as the inset figure shown). Actually, when x is 0 mm, it is the same location as z of 2 mm, and the H is 384 Gs. As the distance from this central point ($x=0$ mm) increases, the surface magnetic intensity decreases. Compared to the surface

magnetic intensity (H) of the cuboid magnet given in Figure 4, the surface magnetic intensity (H) at the central point is large enough to control FF at this designated area.

Next, to simplify the investigation on the effects of some important parameters on the migration behavior, experiments were performed with a permanent magnet, and the average migration distance within 40 s was compared. Figure 6 shows the effect of the volume on the migration distance under various thermal gradients with a gap (h) of 9 mm, and FF-1 is used. When the thermal gradient is $2.0^\circ\text{C}/\text{mm}$, the droplet with a volume of $10\ \mu\text{L}$ migrates in a distance about 14.8 mm, which is longer than the 12.7 mm observed for a volume of $5\ \mu\text{L}$. The migration distance increases with increasing volume of lubricant, and

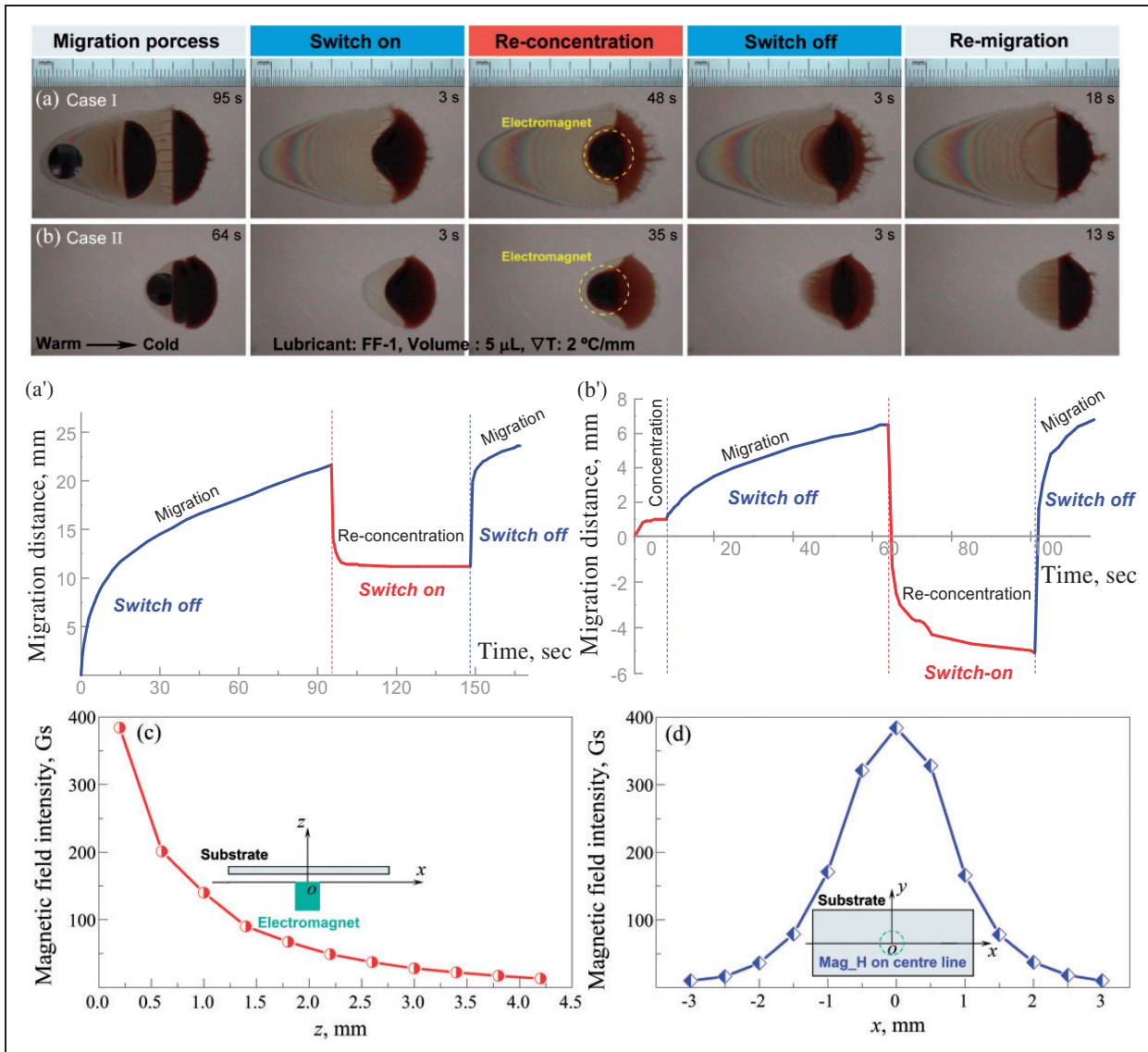


Figure 5. The detailed migration process on a smooth surface including switching on and off operations with droplets placed at different locations: (a) case I, the start position, (b) case II, right above the electromagnet. The detailed migration distance vs elapsed time: (a') case I and (b') case II. (c) The measured surface magnetic intensity (H) at z direction right above the electromagnet center. (d) The measured surface magnetic intensity (H) at the x direction on the substrate surface.

a similar effect is noted under various thermal gradients.

It should be noticed that the increasing volume of a liquid droplet would accelerate the spreading of the liquid on the smooth surface,³² and Wyart and Wasan^{33,34} pointed out that the migration velocity of a liquid droplet due to the thermal gradient is pro-

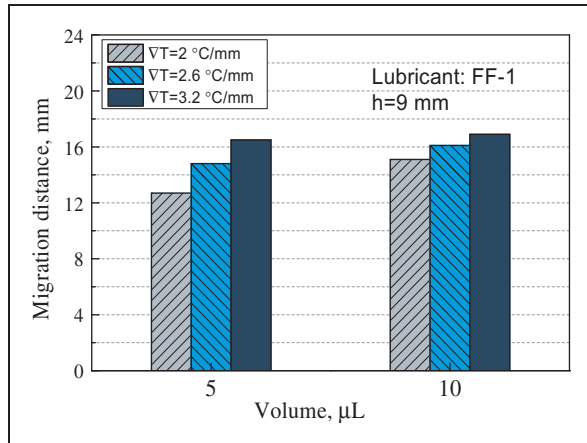


Figure 6. The effect of volume on migration distance under various thermal gradients with an external magnetic field, the gap (h) is 9 mm.

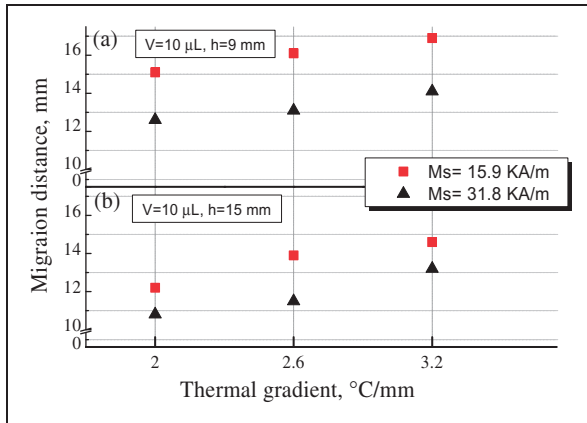


Figure 7. The influence of the saturation magnetization of FF on the migration behavior under various thermal gradients and external magnetic field intensities. (a) $V=10 \mu\text{L}$, $h=9 \text{ mm}$, (b) $V=10 \mu\text{L}$, $h=15 \text{ mm}$.

portional to the droplet height. As the increasing volume will increase the droplet height, the migration distance will be increased.

The saturation magnetization is a vital parameter of FF and its effect on migration behavior is shown in Figure 7. FFs with the saturation magnetization of 15.9 and 31.8 kA/m and a volume of 10 μL are tested. As shown in Figure 7(a), when the gap (h) is 9 mm, under a thermal gradient of 2.0 $^{\circ}\text{C}/\text{mm}$, the FF droplet with the saturation magnetization of 15.9 kA/m migrates in a distance approximately 15.1 mm, which is a little higher than the 12.6 mm observed for the droplet with the saturation magnetization of 31.8 kA/m. The migration distance is decreased with increasing saturation magnetization, and a similar effect is noted under various thermal gradients. Figure 7(b) presents the migration distance when the gap (h) increased to 15 mm. The increasing saturation magnetization of FF always leads to decreased migration distance. It indicates that to achieve a better obstruction effect, FF droplet with a higher saturation magnetization should be employed.

To aid in understanding the mechanism of the migration behavior of the FF droplet, a graphic representation of a FF droplet migrating on an ideal surface under an external magnetic field is shown in Figure 8. The highest magnetic field is at the center location. It is already known that the existence of external magnetic field will generate a magnetic force (F_m) on the droplet. Before the droplet migrating to the center location, the magnetic force contributes to the migration. When the droplet is right upon the center location, the magnetic force (F_m) acts as an adhesive force and fastens the droplet on this location tightly. After the droplet migrates over the location, the magnetic force (F_m) acts as a dragging force resistant to the migration, pulling the droplet back and re-concentrating to the location. Therefore, a sufficiently high magnetic field could control the droplet at designated area firmly, against the thermal capillary force, and a stronger magnetic force (F_m) will be applied on the FF droplet of a higher saturation magnetization, obstructing the migration. Moreover, lubricants with low viscosity are prone to migrate. Therefore, an increased viscosity of the FF due to the external magnetic field could also contribute to the lower migration distance.

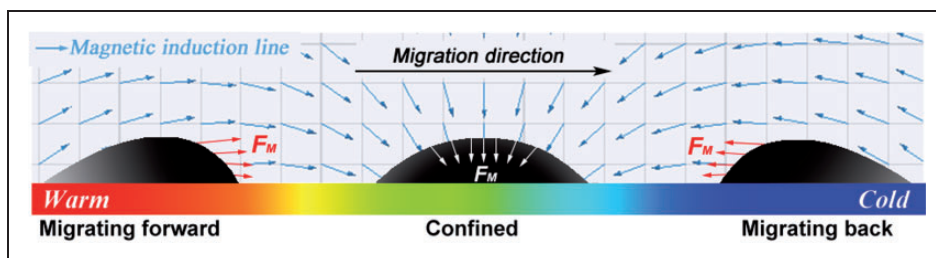


Figure 8. The force exerted on the FF droplets by the external magnetic field and thermal gradient on the ideal surface.

Conclusions

In this study, experiments were carried out to investigate the influence of the external magnetic field on the thermal capillary migration of the FF droplets. An effective technique of using an electromagnet to control the migration and re-concentrate the migrated lubricant was achieved. The conclusions drawn from this study are as follows:

1. The dispersant is indispensable for improving the dispersion performance of the nanoparticles and enhancing the stability of FF; but meanwhile, it will promote the migration behavior.
2. The utilization of FF as lubricant demonstrates a strong anti-migration performance under an external magnetic field.
3. A magnetic switch can be designed to restrict the migration and re-concentrate the migrated FF.
4. FF with higher saturation magnetization can hinder the migration behavior more effectively, and increasing the volume of the ferrofluids will promote the migration.

Declaration of Conflicting Interests

The author(s) declared no potential conflicts of interest with respect to the research, authorship, and/or publication of this article.

Funding

The author(s) disclosed receipt of the following financial support for the research, authorship, and/or publication of this article: This study was supported by the National Natural Science Foundation of China (No. 51475241), Funding for Outstanding Doctoral Dissertation in NUAA (No. BCXJ15-06), and Funding of Jiangsu Innovation Program for Graduate Education (the Fundamental Research Funds for the Central Universities; No. KYLX_0239).

References

1. Levich VG and Krylov VS. Surface-tension-driven phenomena. *Annu Rev Fluid Mech* 1969; 1: 293–316.
2. Brochard F. Motions of droplets on solid surfaces induced by chemical or thermal gradients. *Langmuir* 1989; 5: 432–438.
3. Daniel S, Chaudhury MK and Chen JC. Fast drop movements resulting from the phase change on a gradient surface. *Science* 2001; 291: 633–636.
4. Tadmor R and Pepper KG. Interfacial tension and spreading coefficient for thin films. *Langmuir* 2008; 24: 3185–3190.
5. Subramanian RS, Moumen N and McLaughlin JB. Motion of a drop on a solid surface due to a wettability gradient. *Langmuir* 2005; 21: 11844–11849.
6. Pratap V, Moumen N and Subramanian RS. Thermocapillary motion of a liquid drop on a horizontal solid surface. *Langmuir* 2008; 24: 5185–5193.
7. Tadmor R. Drops that pull themselves up. *Surf Sci* 2014; 628: 17–20.
8. Roberts DW. New frontiers for space tribology. *Tribol Int* 1990; 23: 149–155.
9. Jones WR and Jansen MJ. Tribology for space applications. *Proc IMechE, Part J: J Engineering Tribology* 2008; 222: 997–1004.
10. Sathyan K, Hsu HY, Lee SH, et al. Long-term lubrication of momentum wheels used in spacecrafts - an overview. *Tribol Int* 2010; 43: 259–267.
11. Jones WR, Poslowski AK, Shogrin BA, et al. Evaluation of several space lubricants using a vacuum four-ball tribometer. *Tribol Trans* 1999; 42: 317–323.
12. Cheng T, Zhao B, Chao J, et al. The lubricant migration rate on the hard disk surface. *Tribol Lett* 2001; 9: 181–185.
13. Mettu S and Chaudhury MK. Motion of drops on a surface induced by thermal gradient and vibration. *Langmuir* 2008; 24: 10833–10837.
14. Tadmor R. Approaches in wetting phenomena. *Soft Matter* 2011; 7: 1577–1580.
15. Ke HJ, Huang W and Wang XL. Insights into the effect of thermocapillary migration of droplet on lubrication. *Proc IMechE, Part J: J Engineering Tribology* 2016; 230: 583–590.
16. Sommers AD, Brest TJ and Eid KF. Topography-based surface tension gradients to facilitate water droplet movement on laser-etched copper substrates. *Langmuir* 2013; 29: 12043–12050.
17. Dai QW, Huang W and Wang XL. Surface roughness and orientation effects on the thermo-capillary migration of a droplet of paraffin oil. *Exp Therm Fluid Sci* 2014; 57: 200–206.
18. Zhang P, Liu H, Meng J, et al. Grooved organogel surfaces towards anisotropic sliding of water droplets. *Adv Mater* 2014; 26: 3131–3135.
19. Dai QW, Huang W and Wang XL. Micro-grooves design to modify the thermo-capillary migration of paraffin oil. *Meccanica* 2017; 52: 171–181.
20. Dai QW, Huang W and Wang XL. A surface texture design to obstruct the liquid migration induced by omnidirectional thermal gradients. *Langmuir* 2015; 31: 10154–10160.
21. Wang XL, Wang JQ, Zhang B, et al. Design principles for the area density of dimple patterns. *Proc IMechE, Part J: J Engineering Tribology* 2015; 229: 538–546.
22. Roberts EW and Todd MJ. Space and vacuum tribology. *Wear* 1990; 136: 157–167.
23. Fusaro RL and Khonsari MM. Liquid lubrication for space applications. *NASA TM-105198* 1992.
24. Fannin PC, Marin CN, Malaescu I, et al. An investigation of the microscopic and macroscopic properties of magnetic fluids. *Physica B* 2007; 388: 87–92.
25. Shen C, Huang W, Ma GL, et al. A novel surface texture for magnetic fluid lubrication. *Surf Coat Technol* 2009; 204: 433–439.
26. Rebodos RL and Vikesland PJ. Effects of oxidation on the magnetization of nanoparticulate magnetite. *Langmuir* 2010; 26: 16745–16753.
27. Uhlmann E, Spur G, Bayat N, et al. Application of magnetic fluids in tribotechnical systems. *J Magn Magn Mater* 2002; 252: 336–340.
28. Odenbach S. Recent progress in magnetic fluid research. *J Phys Condens Matter* 2004; 16: 1135–1150.

29. Liao SJ, Huang W and Wang XL. Micro-magnetic field arrayed surface for ferrofluids lubrication. *J Tribol* 2012; 134: 021701–021707.
30. Dai Q, Huang W and Wang X. Insights into the influence of additives on the thermal gradient induced migration of lubricant. *Lubr Sci* 2017; 29: 17–29.
31. Osman TA, Nadab GS and Safar ZS. Effect of using current-carrying-wire models in the design of hydrodynamic journal bearings lubricated with ferrofluid. *Tribol Lett* 2001; 11: 61–70.
32. Bonn D, Eggers J, Indekeu J, et al. Wetting and spreading. *Rev Mod Phys* 2009; 81: 739–805.
33. Brzoska JB, Brochard-Wyart F and Rondelez F. Motions of droplets on hydrophobic model surfaces induced by thermal gradients. *Langmuir* 1993; 9: 2220–2224.
34. Wasan DT, Nikolov AD and Brenner H. Droplets speeding on surfaces. *Science* 2001; 291: 605–606.